Bioconjugate Chemistry

Article

pubs.acs.org/bc

Multiexcitation Fluorogenic Labeling of Surface, Intracellular, and Total Protein Pools in Living Cells

Matharishwan Naganbabu,[†,§] Lydia A. Perkins,[‡,§] Yi Wang,[‡,§] Jeffery Kurish,[†] Brigitte F. Schmidt,[§] and Marcel P. Bruchez*[,†,‡,§]

[†]Department of Chemistry, [‡]Department of Biological Sciences, and [§]Molecular Biosensors and Imaging Center, Carnegie Mellon University, 4400 Fifth Avenue, Pittsburgh 15213, Pennsylvania, United States

Supporting Information

ABSTRACT: Malachite green (MG) is a fluorogenic dye that shows fluorescence enhancement upon binding to its engineered cognate protein, a fluorogen activating protein (FAP). Energy transfer donors such as cyanine and rhodamine dyes have been conjugated with MG to modify the spectral properties of the fluorescent complexes, where the donor dyes transfer energy through Förster resonance energy transfer to the MG complex resulting in binding-conditional fluorescence emission in the far-red region. In this article, we use a violet-excitable dye as a donor to sensitize the far-red emission of the MG-FAP complex. Two blue emitting fluorescent coumarin dyes were coupled to MG and evaluated for energy transfer to the MG-FAP complex via its secondary excitation band. 6,8-Difluoro-7-hydroxycoumarin-3-carboxylic acid (Pacific blue, PB) showed the most efficient energy transfer and maximum brightness in the far-red region upon violet (405 nm) excitation. These blue-red (BluR) tandem dyes are spectrally varied from other tandem dyes and are able to produce fluorescence images of the MG-FAP complex with a large Stokes shift (>250 nm). These dyes are cell-permeable and are used to label intracellular proteins. Used together with a cell-impermeable hexa-Cy3-MG (HCM) dye that labels extracellular proteins, we are able to visualize extracellular, intracellular, and total pools of cellular protein using one fluorogenic tag that combines with distinct dyes to effect different spectral characteristics.

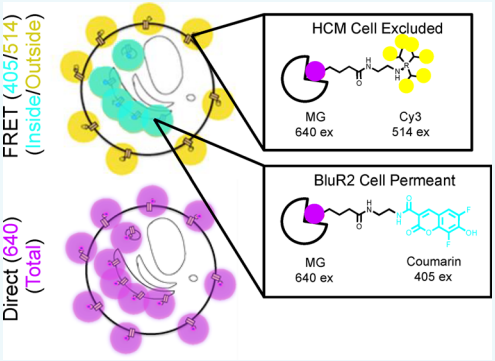

INTRODUCTION

Fluorescence microscopy uses fluorescent labels that absorb and emit light of different wavelengths. The quantitative nature of the fluorescence signal and the ability to achieve visualization of labeled cellular components with high spatiotemporal resolution makes this technique attractive.[1,2] There is a sustained effort to develop different fluorescent labels to enhance our understanding of various cellular components and their functions.[3−6] Fluorescent labels that have a long Stokes shift, are bright, cell permeable, and genetically encodable are preferred for biological imaging.[7]

The development of green fluorescent protein (GFP) as a fluorescent label has spurred tremendous interest in the development of genetically encodable fluorescent labels since it can be used to selectively label a protein of interest (POI) practically and within living cells.[8−10] Despite the development of a blue to near-infrared palette using fluorescent proteins, their brightness and size remain major bottlenecks. Another way of achieving genetic encoding is the use of modifiable amino acids like cysteine or lysine that covalently react with labile functional groups in the fluorescent label.[11,12] While practical for some purified proteins, this approach lacks specificity in the cellular context,[13] and there is an effort to improve selectivity using unnatural amino acids with bio-orthogonal coupling chemistry.[14] A variety of methods use enzymes, either expressed as fusion proteins or preloaded with fluorescent substrates to catalyze covalent ligation of a dye onto an encoded tagging domain on a protein of interest (POI).[15,16] However, for most of these approaches, the background fluorescence due to nonligated labels remains a challenge, requiring a washing step.

An alternate approach to reducing background fluorescence is to use a fluorogenic dye. Fluorogenic dyes have their fluorescence masked until they come in contact with an analyte. Xanthene-based dyes—fluorescein, seminaphthorhodafluor, and rhodamine derivatives have been used as pH responsive fluorogens.[17] Various derivatives of these scaffolds have been used to detect different analytes including metals,[17] reactive oxyen species (ROS),[17] and other biologically relevant substrates.[17−20] To achieve better targeting, recent advances in covalent ligation approaches like the SNAP tag and PYP tag have produced several fluorogenic dye labels as demonstrated by SNAP-SiR,[21,22] SNAP-NileRed,[22] and PYP-dye.[23] However, the fold-activation achieved remains modest.[13]

The development of fluorogen activating proteins (FAPs) that activate otherwise nonfluorescent dyes (fluorogens) upon binding has established a robust fluorogenic activation tagging

Received: March 30, 2016
Revised: May 3, 2016
Published: May 9, 2016

DOI: 10.1021/acs.bioconjchem.6b00169
Bioconjugate Chem. 2016, 27, 1525−1531

approach that functions both *in vitro* and *in vivo*. Single-chain variable fragment (scFv) derived fluorogen activating proteins that bind unsymmetrical cyanine dyes and triarylmethane dyes have shown 10^2-10^4-fold enhancement of the dye fluorescence. In some cases, the ready exchange of the fluorogen in the protein delivers high photostability of the dye−protein complex.[24−26] Further, the brightness of these probes have been enhanced by using Förster resonance energy transfer (FRET) using one or multiple donors in a dendron-like architecture connected to the acceptor fluorogen. The fluorogen activation is achieved by binding the single fluorogen, which otherwise effectively quenches the whole light-harvesting system.[27,28] The genetic encodability of FAP is versatile,[29,30] and we are chemically modifying the fluorogens to achieve a palette of colors.[31−33] Further, FRET has been exploited to develop probes for physiological pH changes,[34] and an expanded suite of energy transfer donors and acceptors[28] will lead to new biosensor options.

FRET is a mechanism by which an excited donor chromophore transfers energy to an acceptor chromophore. The two chromophores should be closely linked, typically well below the Förster radius, to ensure highly efficient energy transfer, and the acceptor excitation must overlap significantly with the donor emission spectra. When the acceptor dye is a constraint-activated fluorogen, as in the case of MG, the FRET pair also shows highly fluorogenic activation upon binding. The low quantum yield of the free fluorogen serves as an efficient quencher of the tandem dye for either direct or FRET-sensitized excitation. Binding of the tandem dye results in activation of the fluorogen acceptor, revealing both direct and FRET-sensitized acceptor fluorescence. Using FRET probes, one can achieve greater Stokes shift and thereby more effectively separate the excitation from the detected emission signal. Long Stokes shift probes are highly desired in biological labeling, allowing rapid detection without splitting the emission pathway in a microscope and enhancing signals relative to cellular autofluorescence.[35,36] Quantum dots,[36,37] lanthanide nanoparticles,[38,39] various dyes[40,41] and fluorescent proteins[3] are available that show large Stokes shifts. Chromophores with long Stokes shift have been employed for applications in super-resolution imaging as well.[42]

Malachite green (MG) is a chromophore with two well-resolved absorbance bands. The primary absorbance band has a λ_{max} of 608 nm, and the secondary absorbance band has a λ_{max} of 468 nm. When MG binds to a fluorogen activating peptide (FAP), dL5**[43] in particular, the λ_{max} of both bands shift bathochromically to 636 and 480 nm, respectively. The noncovalent binding of MG to FAP makes the MG-FAP dye−protein complex fluorescent, and the excitation of either band results in the characteristic far-red fluorescence of the MG-FAP complex.[24,43] Two fluorescent dyes, tetramethyl rhodamine (TMR) and tricarbocyanine (Cy3), have been used to donate energy into the primary absorbance band of the fluorescent MG-FAP dye-protein complex. The fluorogenic FRET dyes were covalent conjugates of donor dyes, TMR and Cy3, that have yellow excitation and emission. We were able to achieve dual-color fluorescence by excitation in the green (514 nm, 532 or 561 nm) and red (640 nm) regions and detection in the far-red (680 nm).[27,28]

Coumarins are benzopyran structures which absorb in the violet region of the visible spectrum and show tunable photophysical properties like quantum yield, extinction coefficient, and photostability.[44−46] These attractive features coupled with the demonstrated utility of coumarins for fluorogenic sensing[47,48] of different analytes and the ability of a donor to transfer energy to a MG-dL5** acceptor prompted us to synthesize coumarin−MG conjugates. In this article, we demonstrate the use of violet-excited, blue-emitting coumarin-based donor dyes for energy transfer into the secondary excitation band of the MG-FAP complex. These tandem dyes are highly fluorogenic, bright and specific labels, enabling dual-excitation measurements with a long Stokes shift. The synthesis, photophysical properties, and cellular labeling studies of these blue-red (BluR) tandem dyes are reported in this article. Further, the applications of these structures in the biological context have been demonstrated by using BluR dyes to selectively label FAP. The fluorescence response of BluR dyes in conjunction with a cell-excluded FAP-fluorogen pair allows visual discrimination of intracellular and extracellular proteins in two distinct FRET channels, while measuring the total protein distribution from the direct MG-FAP excitation. This three-color labeling approach provides quantifiable information about protein distribution in living cells with chemical resolution that exceeds the resolution available by image segmentation or other labeling approaches.[31]

RESULTS AND DISCUSSION

Dye Synthesis. Initially, a commercially available coumarin, 7-hydroxycoumarin-4-acetic acid (7HC), was chosen for the synthesis of the coumarin−MG (BluR1 dye) conjugate. BluR1 was synthesized using amide coupling leading to the formation of a covalent conjugate between coumarin-carboxylic acid and MG[H]EDA, an amine derivative of MG, followed by oxidation to afford the bichromophoric structure. The BluR2 dye was synthesized using the same procedure, in that Pacific blue was used instead of 7-hydroxycoumarin-4-acetic acid.[49] Scheme 1 outlines the process of conjugation of the coumarins and MG. Pacific Blue (PB) was synthesized from 1,3-difluoro-2,4-dimethoxybenzene.[44,50,51] A detailed procedure for the individual dyes is documented in the Supporting Information, section S1.

Spectroscopic Characterization. The absorbance profiles of BluR1 and BluR2, recorded in phosphate buffer saline (PBS) at a pH of 7.4, clearly indicate the conjugation between MG and the respective coumarin. In both the cases, MG does not show any change in its absorbance characteristics (Supporting Information, section S2 and Figure S2.4a). The absorbance maxima for the primary and the secondary absorbance bands of MG in the BluR dyes remains at 608 and 464 nm for the free dye. In the case of BluR1, the 7-hydroxycoumarin-4-acetic acid has an absorbance maximum at 333 nm, a shift from 340 nm in the case of free 7-hydroxycoumarin-4-acetic acid (Supporting Information, section S2 and Figure S2.2). Pacific blue has an absorbance maximum at 420 nm in BluR2, a shift from 385 nm for the free dye in PBS at pH 7.4 (Supporting Information, section S2 and Figure S2.2). MG bound to its cognate FAP dL5** results in a red-shifted absorbance maxima of the primary and the secondary bands from 608 to 636 nm and 464 to 480 nm, respectively. The absorbance peak of 7HC in BluR1 is unaffected by the binding of BluR1 to FAP and continues to be at 333 nm, while in the case of PB (BluR2), the maxima is shifted to 406 nm aligning conveniently with widely available violet lasers in use on confocal microscopes and flow cytometry (Supporting Information, section S2 and Figure S2.5a).

For the measurements of steady-state fluorescence of the BluR dyes, 1 μM dye and 5 μM dL5** were precomplexed for an hour at room temperature in PBS at pH 7.4. The properties of these protein complexes were compared to those of the MG2p-dL5** complex. As a control, a dye only solution

DOI: 10.1021/acs.bioconjchem.6b00169
Bioconjugate Chem. 2016, 27, 1525−1531

Scheme 1. Synthesis of BluR Dyes[a]

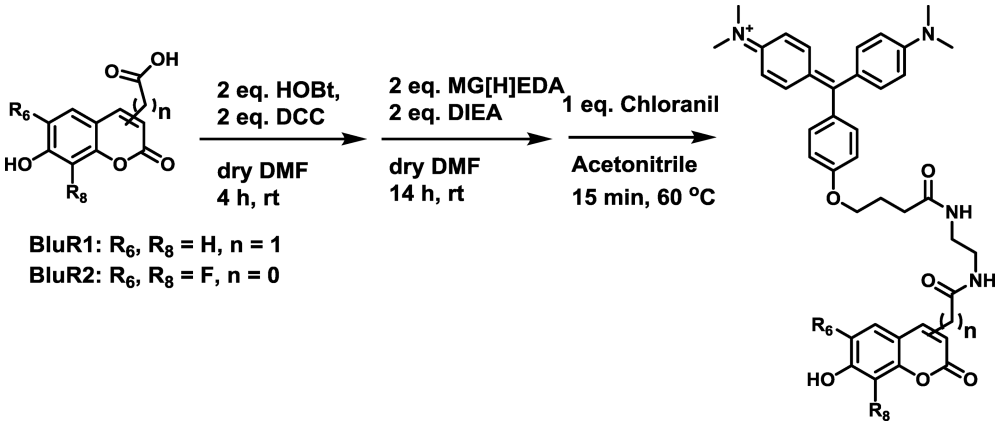

[a]Activation of coumarin-carboxylic acid as a reactive ester using HOBt, DCC followed by coupling using MG[H]EDA, and oxidation of the BluR dye.

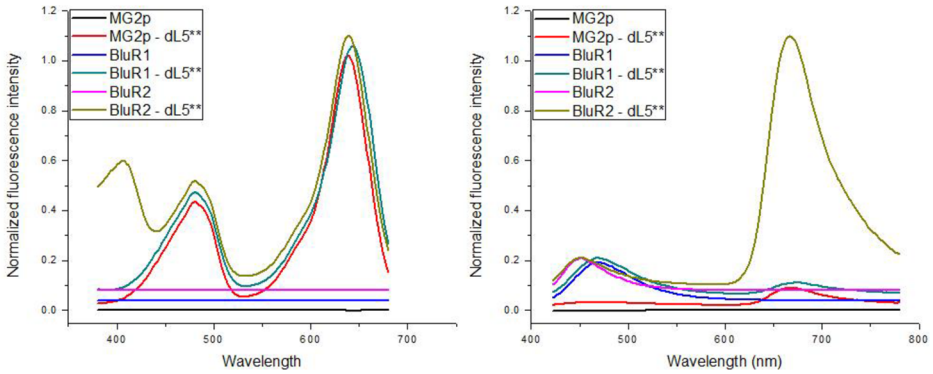

Figure 1. Steady-state fluorescence spectra of BluR dyes recorded using 1 μM dye and 5 μM dL5**. For the excitation spectra (left), the emission wavelength was set to 700 nm, and for the emission spectra (right), the excitation wavelength was set to 405 nm. Excitation spectra have been normalized to the peak with the highest fluorescence intensity for each dye-dL5** complex. Emission spectra are normalized to the peak emission of the BluR2-dL5** complex. The spectra in the figures have each been offset by 0.05 units using Origin 8.0 for clarity.

corresponding to each dye−dL5** complex was prepared. All measurements were carried out on a Photon Technology International (PTI) spectrofluorometer using a slit width of 3 mm corresponding to a spectral bandwidth of 6 nm. Excitation profiles (Figure 1) were recorded from 380 to 670 nm using an λem of 700 nm. BluR1-dL5** and BluR2-dL5** show excitation maxima at 644 and 640 nm, respectively. The excitation profile indicates the presence of a very pronounced coumarin band in BluR2 only. A discernible excitation profile for BluR1-dL5** could not be obtained due to the overlap of second order reflection and the excitation peak. (Supporting Information, section S2 and Figure S2.6b).

The emission profiles were obtained by exciting the BluR-dL5** complexes dyes at two wavelengths. The 405 nm excitation corresponded to an available laser line and enabled energy transfer from the donor coumarin to the acceptor MG-dL5** (Figure 1). The emission maxima for BluR1 and BluR2 were at 672 and 666 nm, respectively (Table 1). BluR2-dL5** was 10-fold brighter than BluR1-dL5** or MG2p-dL5**, indicating that PB is a very good donor under 405 nm excitation. Quantum yield under direct excitation was similar for all dye−dL5** complexes. When excited at 405 nm, BluR1-dL5** showed a maximum of 66-fold enhancement in fluorescence compared to that of BluR1 in the region beyond 600 nm where there is limited to no coumarin fluorescence. This ratio was much higher, at 417-fold, in the case of BluR2-dL5** to BluR2.

The emission profiles of the dyes had similar intensities when excited at 600 nm. Excitation using 600 nm refers to direct excitation of the primary absorbance band of the MG−dL5** complex. The profiles of BluR1−dL5** and BluR2−dL5** are expected to be similar to that of MG−dL5**, the control dye. Accordingly, the emission maxima for BluR1−dL5**, BluR2−dL5**, and MG2p−dL5** were 672, 666, and 666 nm, respectively (Supporting Information, section S2 and Figure S2.8). The spectral properties of BluR2 were similar to those of MG2p, both when free or bound to dL5**. The MG in BluR1 showed a bathochromic shift in absorbance maxima, excitation maxima, and emission maxima. This could be due to the formation of aggregates. We hypothesize that the high pK_a (7.8) of 7HC might enable hydrogen bonding interaction between the dye bound to the dL5** and some polar functional groups present in the dL5**. Nevertheless, it is unusual to see an effect on the MG that is bound in the dL5** pocket. The spectral analysis was not further explored due to the limited utility of probes with UV excitation in biological microscopy.

The energy transfer behavior of the two coumarins, 7-hydroxycoumarin-4-acetic acid and PB, to MG in BluR1−dL5** and BluR2−dL5** were estimated by comparing the coumarin fluorescence intensities of the free or bound BluR dyes and the appropriate coumarin donors (Supporting Information, section S2 and Figures S2.9a and S2.9b) to estimate FRET

DOI: 10.1021/acs.bioconjchem.6b00169
Bioconjugate Chem. 2016, 27, 1525−1531

Table 1. Photophysical Properties of BluR1 and BluR2 Compared to those of MG2p

dye/property	units	BluR1			BluR2			MG2p		
absorbance maxima dye only (1°, 2°, donor)[a]	nm	608	464	333	608	464	420	608	464	n/a
absorbance maxima dye-protein (1°, 2°, donor)[b]	nm	636	481	333	636	480	406	636	480	n/a
excitation maxima (1°, 2°, donor)[c]	nm	640	480	n/a	644	480	408	638	482	n/a
relative excitation (1°, 2°, donor)[c]	nm	1	0.412	n/a	1	0.419	0.499	1	0.416	n/a
emission maxima[d]	nm	672			666			666		
quantum yield[e]		0.2			0.2			0.2		
energy transfer efficiency[f]	%	23.4			95.4					
dissociation constant[g]	nM	<1			<1			<1		

[a]Absorbance was recorded in PBS at pH 7.4. [b]Absorbance was recorded in PBS at pH 7.4 using 5× dL5**. [c]1 μM dye and 5 μM dL5** were used for the measurement of steady-state fluorescence on a PTI instrument with a slit-width of 3 mm corresponding to 6 nm spectral bandwidth. Excitation spectra were measured from 380 nm −670 nm using λem of 700 nm. [d]FRET emission spectra were measured from 420 nm -780 nm using λex: 405 nm. [e]Quantum yield was determined using MG2p-dL5** as a standard. [f]Energy transfer efficiency was determined by comparing the drop in the fluorescence of the donor vs the donor−acceptor-dL5** complex. [g]Dissociation constant (K_d) was determined by titrating dL5** against different concentrations of the dye. Details in Supporting Information, section S3.

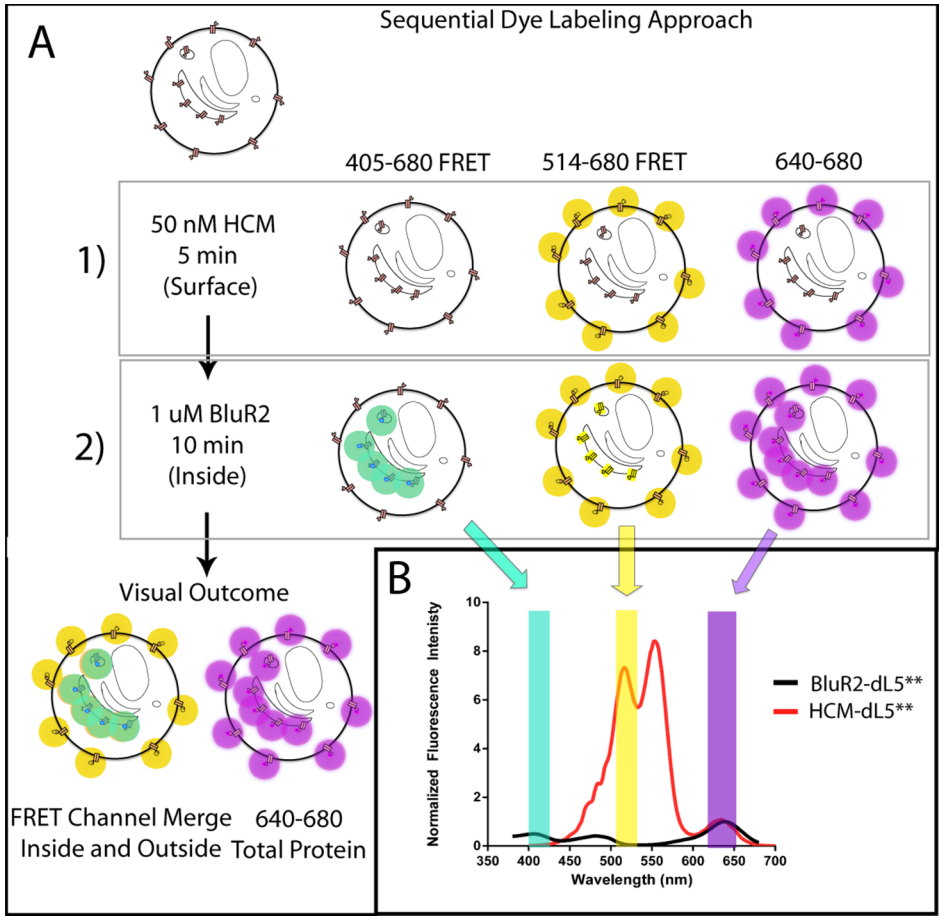

Figure 2. FAP-BKα labeling with HCM and BluR2. (A) Cell surface labeling of FAP-BKα is accomplished with 50 nM cell-impermeable HCM dye for 5 min followed by subsequent labeling of FAP-BKα expressed within the cell with 1 μM cell-permeable BluR2 dye for 10 min. The 640−680 (excitation−emission) column shows the MG signal at each labeling step. The 514−680 column depicts the improvement in signal selectivity for the HCM surface labeling. The 405−680 (excitation−emission) FRET column shows the intracellular labeling of protein with the BluR2 dye. A final FRET channel merge displays the localization of FAP-BKα on the inside and outside of the cell. (B) Spectral properties of the dL5**-BluR2 and HCM complexes used for labeling.

efficiency. Analysis of donor quenching indicated that 7-hydroxycoumarin4-acetic acid was able to transfer only 23.4%, while PB transferred 95.4% of its energy to MG−dL5**. By determining the fluorescence of the dye−dL5** complex (Supporting Information, section S2.10), the quantum yield for both BluR1 and BluR2 was calculated to be 0.20, the same as that of the standard. The quantum yield of MG2p−dL5** was previously obtained by comparison with Cy5.18 as a reference fluorophore.[43] The binding affinities of the BluR dyes to dL5** were in the same range as that of MG2p−dL5** indicating no significant perturbation in the binding behavior of MG to dL5** due to the presence of the coumarin (Table1). A detailed explanation of the method used can be found in Supporting Information, section S3.

DOI: 10.1021/acs.bioconjchem.6b00169
Bioconjugate Chem. 2016, 27, 1525−1531

BluR2−dL5** is a superior FRET tandem dye, both *in vitro* and *in vivo*, as compared to BluR1−dL5**. The subtle differences in the structure and the chemical composition of the donor coumarin play an important role in determining the energy transfer behavior of the dyes. On the basis of the spectral properties, these dyes are expected to show similar Förster radii (~50 Å), but E values were markedly different. A detailed explanation of the procedure used to calculate the Förster radii is described in Supporting Information, section S2.3. The presence of 3-carboxylic acid red-shifts the absorbance maximum[44,52] providing a large excitation cross-section at 405 nm which corresponds to a commercially available laser line. Other laser sources (e.g., 355 or 375 nm) that can be used to excite coumarin dye might result in greater cellular toxicity. Further, the fluorescence behavior and energy transfer abilities depend largely on the ability of the coumarin to be in an excitable state. In this case, the 7-hydroxy group should exist as an anion to be efficiently excited. Since all measurements were carried out in a pH of 7.4, pK_a plays an important role. The pK_a of the 7-hydroxy group in 7HC is 7.8,[53] while in the case of PB the pK_a is 3.7.[52] The two fluorines ortho to the 7-hydroxy group are electron withdrawing in nature and make it more acidic. As a result, PB would be in a near-complete anionic state at a pH of 7.4, while 7HC would be just 30%. Under the basic conditions (pH > 8) required to activate the 7-HC, the MG chromophore is decolorized by carbinol formation, resulting in reduced donor quenching, reduced FAP binding, and no fluorescence activaton, precluding the determination of the pH dependence of FAP-fluorogen spectral properties for this dye.[54] We tested the absorbance of BluR1 (only) from pH 7−9 and found that the coumarin band increased and shifted to ~375 nm under alkaline conditions (Supporting Information, section S2.4c) The binding affinities of the BluR dyes and MG2p are comparable (Supporting Information, section S3) indicating no effect on the binding of MG to dL5** due to the presence of a donor coumarin. This is in agreement with the crystal structure data that indicates the linker to be projecting well-outside the binding pocket of dL5**.[43]

Cellular Imaging. The large Stokes shift of BluR2−dL5**, greater than 250 nm, allows multicolor FRET FAP labeling to identify protein localization while using MG (640−680) fluorescence to image total FAP tagged protein. To demonstrate an *in vivo* application of BluR2, sequential dye labeling was employed to gain a representative visualization of protein expressed within a cell and on the cell surface. The inside/outside cellular model used the expression of the large conductance, voltage-and calcium-activated potassium (BK) channel, which has pronounced BK channel expression intracellularly and on the plasma membrane. The dL5** FAP-BKα fusion construct has been previously established and validated in HEK-293 cells.[31] The initial labeling of FAP-BKα at the cell surface was achieved with Hexa-Cy3-MG (HCM) dye,[55] a cell impermeable dyedron, consisting of six Cy3 dyes linked to one MG fluorogen. Each Cy3 dye is negatively charged making the dyedron robustly cell-excluded. Coumarin and monocationic MG in BluR2 make the dye zwitterionic and as a result cell permeable. After preincubation with HCM to label the cell surface population of dL5**, FAP-BKα BluR2 was subsequently used to label the intracellular protein (Figure 2). This two dye labeling procedure uses simple dye additions without any media removal or wash steps. Use of 514 excitation, where MG excitation is minimal, provides excitation selectivity and is used in lieu of 560 nm for Cy3-MG FRET fluorescence (Figure 3 and Supporting Information, section S4).

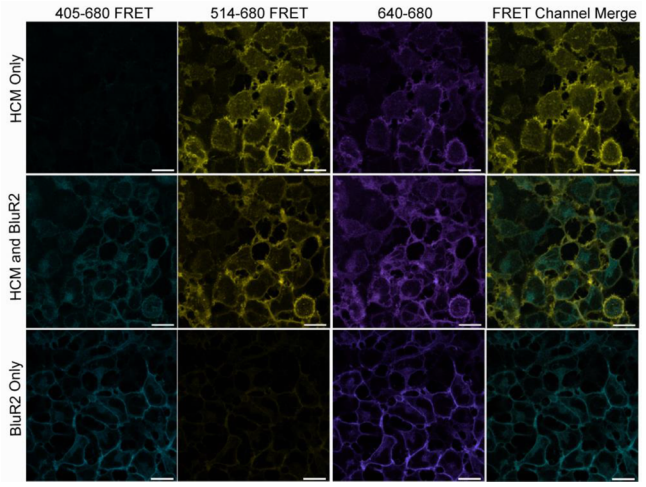

Figure 3. Result of surface and intracellular labeling of FAP-BKα expressing HEK-293 cells. The HCM only row shows surface labeling and low 405−680 (excitation−emission) fluorescence. BluR2 only presents total protein labeling (outside and inside). The 514−680 FRET channel of BluR2 shows low signal. In the HCM and BluR2 row, the 640−680 (excitation−emission) panel depicts total protein, and the last panel of the FRET channels exhibits the merge of the 514−680 and 405−680 fluorescence. The FRET channel merge gives a visual representation of protein expressed on the surface, shown by the strong yellow signal, and the protein present in the inside is represented by the cerulean fluorescence. Scale bar: 20 μm.

CONCLUSIONS

In conclusion, we have developed a new class of fluorogenic, long Stokes shift tandem dyes that binds to a fluorescence activating protein. The tandem dye allows for imaging cellular proteins using two different channels, 405 and 640 nm. Also, the large fluorescence activation eliminates the need for a wash step during imaging. BluR2, a cell-permeable dye, was used in sequential labeling with another fluorogenic dye, HCM, to selectively label extracellular and intracellular pools of protein, allowing excitation-dependent visualization of extracellular, intracellular, and total protein pools in the same cells. The establishment of coumarin as a donor that can be excited orthogonally provides significant opportunities for the development of a series of probes for different analytes by exploiting the chromogenic behavior of the 7-hydroxyl group.

ASSOCIATED CONTENT

Supporting Information

The Supporting Information is available free of charge on the ACS Publications website at DOI: 10.1021/acs.bioconjchem.6b00169.

Synthesis and characterization of BluR dyes; photophysical properties of BluR dyes; binding affinity of BluR dyes; and cell imaging of BluR dyes (PDF)

AUTHOR INFORMATION

Corresponding Author

*E-mail: bruchez@cmu.edu.

Notes

The authors declare the following competing financial interest(s): M.P.B. is a founder of and holds equity in Sharp Edge Labs, a company commercializing the FAP-fluorogen technology.

DOI: 10.1021/acs.bioconjchem.6b00169
Bioconjugate Chem. 2016, 27, 1525−1531

■ ACKNOWLEDGMENTS

This work was supported by NIH grant R01EB017268 (to M.N., Y.W., B.F.S., and M.P.B.), and a Carnegie Mellon University Presidential Fellowship (to L.A.P.). We thank Dr. Cheryl Telmer and Dr. Mingrui Zhang for their input on the protein synthesis and Chris Pratt for FAP-BK expressing HEK293 cells.

■ REFERENCES

(1) Kentner, D., and Sourjik, V. (2010) Use of fluorescence microscopy to study intracellular signaling in bacteria. *Annu. Rev. Microbiol. 64*, 373−390.

(2) Jing, C., and Cornish, V. W. (2011) Chemical tags for labeling proteins inside living cells. *Acc. Chem. Res. 44*, 784−792.

(3) Wu, B., Piatkevich, K. D., Lionnet, T., Singer, R. H., and Verkhusha, V. V. (2011) Modern fluorescent proteins and imaging technologies to study gene expression, nuclear localization, and dynamics. *Curr. Opin. Cell Biol. 23*, 310−317.

(4) Tantama, M., Hung, Y. P., and Yellen, G. (2011) Imaging intracellular pH in live cells with a genetically encoded red fluorescent protein sensor. *J. Am. Chem. Soc. 133*, 10034−10037.

(5) Revelo, N. H., Kamin, D., Truckenbrodt, S., Wong, A. B., Reuter-Jessen, K., Reisinger, E., Moser, T., and Rizzoli, S. O. (2014) A new probe for super-resolution imaging of membranes elucidates trafficking pathways. *J. Cell Biol. 205*, 591−606.

(6) Dodani, S. C., Leary, S. C., Cobine, P. A., Winge, D. R., and Chang, C. J. (2011) A targetable fluorescent sensor reveals that copper-deficient SCO1 and SCO2 patient cells prioritize mitochondrial copper homeostasis. *J. Am. Chem. Soc. 133*, 8606−8616.

(7) Shank, N. I., Pham, H. H., Waggoner, A. S., and Armitage, B. A. (2013) Twisted cyanines: a non-planar fluorogenic dye with superior photostability and its use in a protein-based fluoromodule. *J. Am. Chem. Soc. 135*, 242−251.

(8) Shaner, N. C., Steinbach, P. A., and Tsien, R. Y. (2005) A guide to choosing fluorescent proteins. *Nat. Methods 2*, 905−909.

(9) Yan, Q., and Bruchez, M. P. (2015) Advances in chemical labeling of proteins in living cells. *Cell Tissue Res. 360*, 179−194.

(10) Giepmans, B. N., Adams, S. R., Ellisman, M. H., and Tsien, R. Y. (2006) The fluorescent toolbox for assessing protein location and function. *Science 312*, 217−224.

(11) Hoffmann, C., Gaietta, G., Zürn, A., Adams, S. R., Terrillon, S., Ellisman, M. H., Tsien, R. Y., and Lohse, M. J. (2010) Fluorescent labeling of tetracysteine-tagged proteins in intact cells. *Nat. Protoc. 5*, 1666−1677.

(12) Asano, S., Patterson, J. T., Gaj, T., and Barbas, C. F. (2014) Site-selective labeling of a lysine residue in human serum albumin. *Angew. Chem., Int. Ed. 53*, 11783−11786.

(13) Bruchez, M. P. (2015) Dark dyes-bright complexes: fluorogenic protein labeling. *Curr. Opin. Chem. Biol. 27*, 18−23.

(14) Shieh, P., and Bertozzi, C. R. (2014) Design strategies for bioorthogonal smart probes. *Org. Biomol. Chem. 12*, 9307−9320.

(15) Los, G. V., Encell, L. P., McDougall, M. G., Hartzell, D. D., Karassina, N., Zimprich, C., Wood, M. G., Learish, R., Ohana, R. F., Urh, M., et al. (2008) HaloTag: a novel protein labeling technology for cell imaging and protein analysis. *ACS Chem. Biol. 3*, 373−382.

(16) Stagge, F., Mitronova, G. Y., Belov, V. N., Wurm, C. A., and Jakobs, S. (2013) SNAP-, CLIP- and Halo-tag labelling of budding yeast cells. *PLoS One 8*, e78745.

(17) Li, X., Gao, X., Shi, W., and Ma, H. (2014) Design strategies for water-soluble small molecular chromogenic and fluorogenic probes. *Chem. Rev. 114*, 590−659.

(18) Holmes, C. P., Macher, N., Grove, J. R., Jang, L., and Irvine, J. D. (2008) Designing better coumarin-based fluorogenic substrates for PTP1B. *Bioorg. Med. Chem. Lett. 18*, 3382−3385.

(19) Rong, L., Liu, L. H., Chen, S., Cheng, H., Chen, C. S., Li, Z. Y., Qin, S. Y., and Zhang, X. Z. (2014) A coumarin derivative as a fluorogenic glycoproteomic probe for biological imaging. *Chem. Commun. (Cambridge, U. K.) 50*, 667−669.

(20) Shieh, P., Dien, V. T., Beahm, B. J., Castellano, J. M., Wyss-Coray, T., and Bertozzi, C. R. (2015) CalFluors: A Universal Motif for Fluorogenic Azide Probes across the Visible Spectrum. *J. Am. Chem. Soc. 137*, 7145−7151.

(21) Lukinavičius, G., Umezawa, K., Olivier, N., Honigmann, A., Yang, G., Plass, T., Mueller, V., Reymond, L., Corrêa, I. R., Luo, Z. G., et al. (2013) A near-infrared fluorophore for live-cell super-resolution microscopy of cellular proteins. *Nat. Chem. 5*, 132−139.

(22) Prifti, E., Reymond, L., Umebayashi, M., Hovius, R., Riezman, H., and Johnsson, K. (2014) A fluorogenic probe for SNAP-tagged plasma membrane proteins based on the solvatochromic molecule Nile Red. *ACS Chem. Biol. 9*, 606−612.

(23) Hori, Y., Ueno, H., Mizukami, S., and Kikuchi, K. (2009) Photoactive yellow protein-based protein labeling system with turn-on fluorescence intensity. *J. Am. Chem. Soc. 131*, 16610−16611.

(24) Szent-Gyorgyi, C., Schmidt, B. F., Creeger, Y., Fisher, G. W., Zakel, K. L., Adler, S., Fitzpatrick, J. A., Woolford, C. A., Yan, Q., Vasilev, K. V., et al. (2008) Fluorogen-activating single-chain antibodies for imaging cell surface proteins. *Nat. Biotechnol. 26*, 235−240.

(25) Saurabh, S., Zhang, M., Mann, V. R., Costello, A. M., and Bruchez, M. P. (2015) Kinetically Tunable Photostability of Fluorogen-Activating Peptide-Fluorogen Complexes. *ChemPhysChem 16*, 2974−2980.

(26) Plamont, M. A., Billon-Denis, E., Maurin, S., Gauron, C., Pimenta, F. M., Specht, C. G., Shi, J., Quérard, J., Pan, B., Rossignol, J., et al. (2016) Small fluorescence-activating and absorption-shifting tag for tunable protein imaging in vivo. *Proc. Natl. Acad. Sci. U. S. A. 113*, 497−502.

(27) Szent-Gyorgyi, C., Schmidt, B. F., Fitzpatrick, J. A., and Bruchez, M. P. (2010) Fluorogenic dendrons with multiple donor chromophores as bright genetically targeted and activated probes. *J. Am. Chem. Soc. 132*, 11103−11109.

(28) Yushchenko, D. A., Zhang, M., Yan, Q., Waggoner, A. S., and Bruchez, M. P. (2012) Genetically targetable and color-switching fluorescent probe. *ChemBioChem 13*, 1564−1568.

(29) Yan, Q., Schmidt, B. F., Perkins, L. A., Naganbabu, M., Saurabh, S., Andreko, S. K., and Bruchez, M. P. (2015) Near-instant surface-selective fluorogenic protein quantification using sulfonated triarylmethane dyes and fluorogen activating proteins. *Org. Biomol. Chem. 13*, 2078−2086.

(30) Telmer, C. A., Verma, R., Teng, H., Andreko, S., Law, L., and Bruchez, M. P. (2015) Rapid, specific, no-wash, far-red fluorogen activation in subcellular compartments by targeted fluorogen activating proteins. *ACS Chem. Biol. 10*, 1239−1246.

(31) Pratt, C. P., He, J., Wang, Y., Barth, A. L., and Bruchez, M. P. (2015) Fluorogenic Green-Inside Red-Outside (GIRO) Labeling Approach Reveals Adenylyl Cyclase-Dependent Control of BKα Surface Expression. *Bioconjugate Chem. 26*, 1963−1971.

(32) Zhang, M., Chakraborty, S. K., Sampath, P., Rojas, J. J., Hou, W., Saurabh, S., Thorne, S. H., Bruchez, M. P., and Waggoner, A. S. (2015) Fluoromodule-based reporter/probes designed for in vivo fluorescence imaging. *J. Clin. Invest. 125*, 3915−3927.

(33) Zanotti, K. J., Silva, G. L., Creeger, Y., Robertson, K. L., Waggoner, A. S., Berget, P. B., and Armitage, B. A. (2011) Blue fluorescent dye-protein complexes based on fluorogenic cyanine dyes and single chain antibody fragments. *Org. Biomol. Chem. 9*, 1012−1020.

(34) Grover, A., Schmidt, B. F., Salter, R. D., Watkins, S. C., Waggoner, A. S., and Bruchez, M. P. (2012) Genetically encoded pH sensor for tracking surface proteins through endocytosis. *Angew. Chem., Int. Ed. 51*, 4838−4842.

(35) Aubin, J. E. (1979) Autofluorescence of viable cultured mammalian cells. *J. Histochem. Cytochem. 27*, 36−43.

(36) Resch-Genger, U., Grabolle, M., Cavaliere-Jaricot, S., Nitschke, R., and Nann, T. (2008) Quantum dots versus organic dyes as fluorescent labels. *Nat. Methods 5*, 763−775.

DOI: 10.1021/acs.bioconjchem.6b00169
Bioconjugate Chem. 2016, 27, 1525−1531

(37) Saurabh, S., Beck, L. E., Maji, S., Baty, C. J., Wang, Y., Yan, Q., Watkins, S. C., and Bruchez, M. P. (2014) Multiplexed modular genetic targeting of quantum dots. *ACS Nano 8*, 11138−11146.
(38) Hanaoka, K., Kikuchi, K., Kojima, H., Urano, Y., and Nagano, T. (2004) Development of a zinc ion-selective luminescent lanthanide chemosensor for biological applications. *J. Am. Chem. Soc. 126*, 12470−12476.
(39) Wang, F., and Liu, X. (2014) Multicolor tuning of lanthanide-doped nanoparticles by single wavelength excitation. *Acc. Chem. Res. 47*, 1378−1385.
(40) Lavis, L. D., and Raines, R. T. (2014) Bright building blocks for chemical biology. *ACS Chem. Biol. 9*, 855−866.
(41) Lin, W., Yuan, L., Cao, Z., Feng, Y., and Song, J. (2010) Through-bond energy transfer cassettes with minimal spectral overlap between the donor emission and acceptor absorption: coumarin-rhodamine dyads with large pseudo-Stokes shifts and emission shifts. *Angew. Chem., Int. Ed. 49*, 375−379.
(42) Nizamov, S., Willig, K. I., Sednev, M. V., Belov, V. N., and Hell, S. W. (2012) Phosphorylated 3-heteroarylcoumarins and their use in fluorescence microscopy and nanoscopy. *Chem. - Eur. J. 18*, 16339−16348.
(43) Szent-Gyorgyi, C., Stanfield, R. L., Andreko, S., Dempsey, A., Ahmed, M., Capek, S., Waggoner, A., Wilson, I. A., and Bruchez, M. P. (2013) Malachite green mediates homodimerization of antibody VL domains to form a fluorescent ternary complex with singular symmetric interfaces. *J. Mol. Biol. 425*, 4595−4613.
(44) Sun, W. C., Gee, K. R., and Haugland, R. P. (1998) Synthesis of novel fluorinated coumarins: excellent UV-light excitable fluorescent dyes. *Bioorg. Med. Chem. Lett. 8*, 3107−3110.
(45) Surya Prakash Rao, H., Babu, M., and Desai, A. (2014) Synthesis, characterization and spectroscopic properties of water soluble coumarins substituted with oligomeric alkoxy functions. *RSC Adv. 4*, 11064.
(46) Long, L., Li, X., Zhang, D., Meng, S., Zhang, J., Sun, X., Zhang, C., Zhou, L., and Wang, L. (2013) Amino-coumarin based fluorescence ratiometric sensors for acidic pH and their application for living cells imaging. *RSC Adv. 3*, 12204.
(47) Yuan, L., Lin, W., Xie, Y., Chen, B., and Zhu, S. (2012) Single fluorescent probe responds to H2O2, NO, and H2O2/NO with three different sets of fluorescence signals. *J. Am. Chem. Soc. 134*, 1305−1315.
(48) Long, S., Chen, L., Xiang, Y., Song, M., Zheng, Y., and Zhu, Q. (2012) An activity-based fluorogenic probe for sensitive and selective monoamine oxidase-B detection. *Chem. Commun. (Cambridge, U. K.) 48*, 7164−7166.
(49) Pisani, L., Muncipinto, G., Miscioscia, T. F., Nicolotti, O., Leonetti, F., Catto, M., Caccia, C., Salvati, P., Soto-Otero, R., Mendez-Alvarez, E., et al. (2009) Discovery of a novel class of potent coumarin monoamine oxidase B inhibitors: development and biopharmacological profiling of 7-[(3-chlorobenzyl)oxy]-4-[(methylamino)-methyl]-2H-chromen-2-one methanesulfonate (NW-1772) as a highly potent, selective, reversible, and orally active monoamine oxidase B inhibitor. *J. Med. Chem. 52*, 6685−6706.
(50) Hedberg, C., Dekker, F. J., Rusch, M., Renner, S., Wetzel, S., Vartak, N., Gerding-Reimers, C., Bon, R. S., Bastiaens, P. I., and Waldmann, H. (2011) Development of highly potent inhibitors of the Ras-targeting human acyl protein thioesterases based on substrate similarity design. *Angew. Chem., Int. Ed. 50*, 9832−9837.
(51) Orange, C., Specht, A., Puliti, D., Sakr, E., Furuta, T., Winsor, B., and Goeldner, M. (2008) Synthesis and photochemical properties of a light-activated fluorophore to label His-tagged proteins. *Chem. Commun. (Cambridge, U. K.) 10*, 1217−1219.
(52) Cohen, J. D., Thompson, S., and Ting, A. Y. (2011) Structure-guided engineering of a Pacific Blue fluorophore ligase for specific protein imaging in living cells. *Biochemistry 50*, 8221−8225.
(53) Chilvers, K. F., Perry, J. D., James, A. L., and Reed, R. H. (2001) Synthesis and evaluation of novel fluorogenic substrates for the detection of bacterial beta-galactosidase. *J. Appl. Microbiol. 91*, 1118−1130.
(54) Jin, X., Uttamapinant, C., and Ting, A. Y. (2011) Synthesis of 7-aminocoumarin by Buchwald-Hartwig cross coupling for specific protein labeling in living cells. *ChemBioChem 12*, 65−70.
(55) Wang, Y., Telmer, C. A., Schmidt, B. F., Franke, J. D., Ort, S., Arndt-Jovin, D. J., and Bruchez, M. P. (2015) Fluorogen activating protein-affibody probes: modular, no-wash measurement of epidermal growth factor receptors. *Bioconjugate Chem. 26*, 137−144.

DOI: 10.1021/acs.bioconjchem.6b00169
Bioconjugate Chem. 2016, 27, 1525−1531